Chapter 3. Static Non-Linear Beam Bending Analysis

In this chapter we revisit non-linear beam bending analysis, with the objective of understanding the basic attributes of flexure units. The reason for choosing a uniform beam is that it is one of the most common flexure elements, and at the same time is simple enough to allow for closed-form analysis. Based on the results of this analysis, we seek insights into the nature of concepts such as Degrees of Freedom, parasitic error, over-constraint and stiffness variation with displacements. Once this is done, we shall have the tools and terminology to investigate other more complex flexure elements and mechanisms. While thermal effects can play an important role in the performance of flexures, we limit our present analysis to only the structural aspects. Furthermore, although an explicit dynamic analysis is not performed at this stage, some key conclusions pertaining to the dynamic performance may be obtained from the results of the static analysis.

All the attributes and performance measures of interest, as outlined in Chapters 1 and 2, can be derieved from the force displacement characteristics of a given flexure unit. Therefore, based on the principles of solid mechanics, we proceed to analyze these characteristics for the simple beam flexure. A typical formulation in mechanics consists of three components [69-70]

a) Constitutive relationships
b) Force equilibrium or force compatibility relationships
c) Geometric equilibrium or geometric compatibility relationships

All three of the above relationships determine the overall nature of a problem, for example, whether the formulation will be linear or non-linear. Non-linearity in a formulation may be a consequence of either of the above.

At the macro scale, constitutive relationships relate loads to deformations. For an infinitesimally small differential element, these relationships relate the stresses to strain, and are dependent on the material properties.

Force equilibrium is commonly applied to a loaded elastic body in its undeformed configuration, but in reality, forces are truly in equilibrium only in the deformed configuration. Since the deformations are small, it is usually assumed that force equilibrium equations will not be affected significantly irrespective of whether they are applied in the deformed or undeformed configuration. While this a reasonable assumption for many cases, there are other situations where force equilibrium in the system is critically dependent on the deformation that results from the forces on the system, for example, during a transverse

displacement of a string under tension. It is important to realize that, in such situations, even though force equilibrium conditions may include the non-linearities arising from displacement variables, these equations are necessarily linear in the load terms, as required by Newton's Laws.

Furthermore, systems obey certain geometric constraints which results in the conditions of geometric compatibility or geometric equilibrium. In almost all cases, geometric compatibility is a purely kinematic relationship, often non-linear in the displacement variables, but independent of loads. But this should not be mistaken for a rule. Although uncommon, there are cases, where geometric compatibility becomes dependent on the loading. Such a situation, and its consequence on the elastic analysis, is discussed later in this chapter.

A given mechanics problem may be approached by explicitly solving the equations resulting from all three of the above relationships simultaneously. This involves the internal forces and displacements, which may not be of interest as far as the final results are concerned. Energy methods arising from the Principles of Virtual Work and Complimentary Virtual work offer a computationally efficient, and mathematically elegant alternative to the former approach. While all analysis in this chapter is done using the former approach, a discussion on the applicability and use of energy methods in this context is presented towards the end.

Finally, to be able to employ the principles of mechanics to achieve relationships that are useful for flexure design, and at the same time are accurate enough, several carefully justified engineering approximation need to made. One of the key steps in this analysis is recognizing what effects are important and what are not. This is achieved by making use of engineering judgment, mathematical insight and non-dimensional analysis.

3.1 Beam Bending Analysis

Classical beam bending analysis is commonly found in several undergraduate and advanced texts [69-71]. These derivations are based on a formulation that is attributed to Jacob Bernoulli and Leonard Euler [72]. Although the final results of Bernoulli's original analysis are known to be erroneous, the basic assumptions that he made are very powerful and hence constitute the starting point in classical beam bending theory.

Since we would like to study secondary effects resulting from axial forces in a beam, it is important to verify the validity of Bernoulli's assumptions. Fundamentally, these assumptions are based on arguments of symmetry. One can imagine an infinitely long slender beam with a uniform rectangular cross-section subjected to a pure bending moment. Consider a finite length segment of this beam centered about axis *O*-

O, in an undeformed and a deformed configuration, shown in Figures 3.1A and 3.1B, respectively. At this stage, no assumptions are made regarding either the height or depth of the beam.

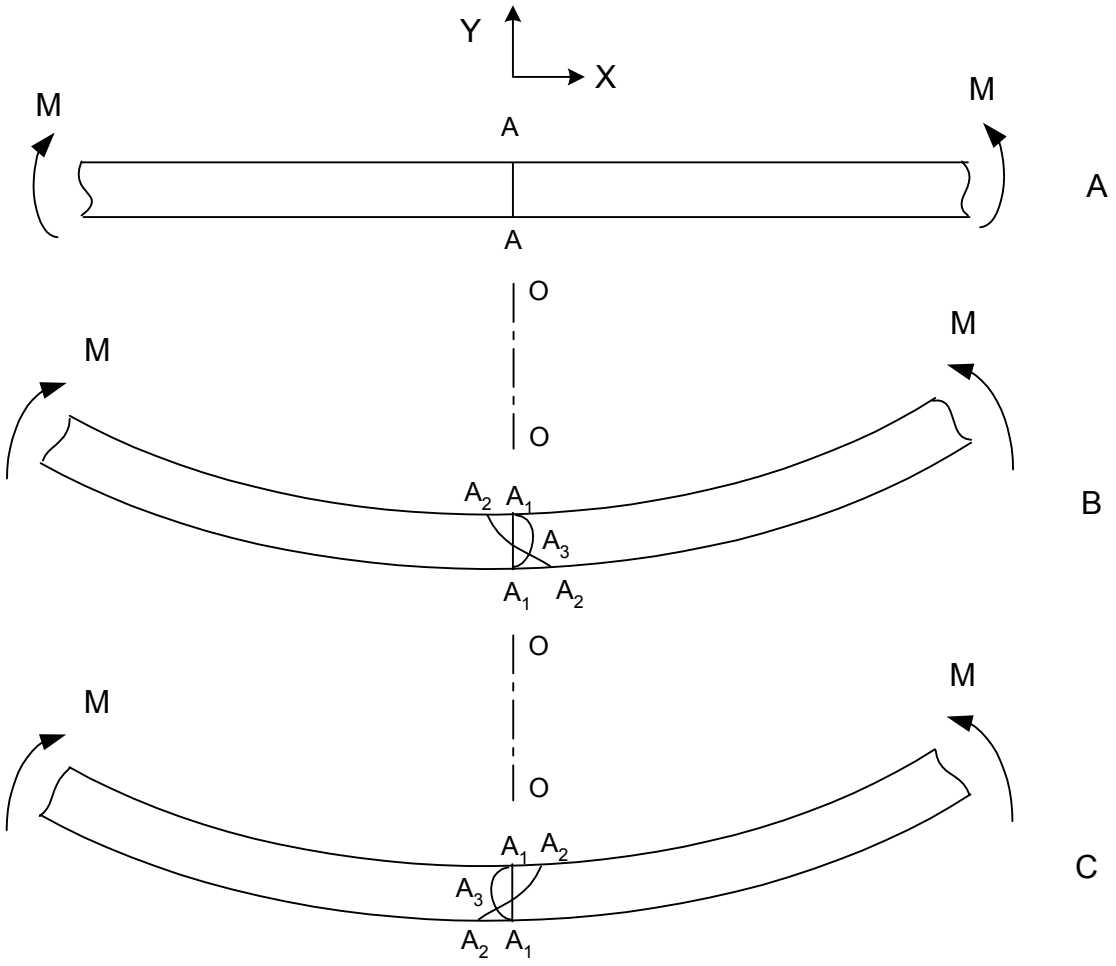

Fig.3.1 Infinite beam under pure moment load

Now let us reason what happens to a cross-section plane A-A that is initially aligned along the O-O axis in the undeformed beam. After deformation, the section A-A can assume one of several possible configurations for example, A_1, A_2 or A_3. It is easily seen from Fig. 3.1B that the loading and the geometry of the beam are perfectly symmetrical about the O-O axis. Therefore, if one flips the beam about the O-O axis, since the loading and external geometry of the beam remain unchanged, all the beam cross-sections in their deformed configuration should appear as though nothing changed. This argument rules out all possibilities like A_2 and A_3. The only post deformation configuration of A-A that withstands the above requirements of symmetry is A_1. Based on this simple mental experiment, one can make two conclusions,

a) Plane sections remain plane after deformation
b) Plane sections remain normal to the top and bottom faces of the beam after deformation

The above set of arguments, and therefore the resulting conclusions, do not change if one chooses a different cross-section, as along as it is uniform and symmetric. More importantly, the presence of a uniform axial force along the beam doesn't affect these conclusions either.

For practical reasons, beams are not infinite. But a slender beam with a height much smaller in comparison to the length, is a close approximation. In this case, from the point of view of a cross-section in the beam, which is far away from either end, the beam appears *almost* infinite. The above arguments also assume that moment is constant along the length of the beam, which is clearly not the case when a shear force is present. Since shear forces break the loading symmetry, one would doubt the above conclusions. But once again, for small beam heights, variations in moment over the length of the beam do not appear very significant, and these conclusions may still be used as very good engineering approximations. In fact, finite element analysis and experimental evidence corroborates the validity of these approximations.

As the beam height is increased, one may no longer be able to treat the beam as being infinitely long, and therefore the approximations start to fail, and plane sections no longer remain plane. In this case, pursuing beam bending analysis based on Bernoulli's assumptions results in the contradictory situation where shear strains are zero, while the shear stresses are finite and large. This anomaly is elegantly resolved in Timoshenko's beam bending theory [71]. Although, physically less intuitive, Timoshenko's formulation provides a more accurate representation of non-slender beams, owing to its mathematical rigor.

Typically for flexure elements the height is kept significantly smaller than the length, and therefore Bernoulli's assumptions hold. Furthermore, even when the cross-sections warp, the final results of the classical beam bending theory stay valid as long as the axial and the shear forces remain constant [70], which is often the case.

Euler further made the assumption that apart from being thin in the Y direction, the beam is also thin in the Z direction. This then allows for a plane stress assumption in the XY and XZ planes. Commonly, in the case of flexures, a relatively large Z dimension is used to limit motion to the XY plane. In that case, it can be shown that the strains in the Z direction are negligibly small, resulting in plane strain in the XY plane, while the XZ plane still remains in plane stress. Thus, depending upon the Z dimension of the beam, the XY plane will either be in a state of plane stress or plane strain. For either case, the analysis that follows is straight forward. We simply state the final result, which applies at every cross-section of the beam, and is commonly known as *Euler's formula*.

$$\frac{E}{\rho} = \frac{M}{I} \tag{3.1}$$

where,

M is the moment at a given cross-section in the beam, I is the second moment of area about the Z axis, ρ is the radius of curvature, and

$E = E^*$ if Plane Stress

$= E^* / (1 - \nu^2)$ if Plane Strain, and

E^* and v are the Young's modulus and Poisson's ratio of the material, respectively.

As we proceed through this analysis, there are several approximations that we will need to make, and these are appropriately justified wherever mentioned. To be able to make any decisions regarding dropping of terms, we should have an idea of the maximum amount of motion and forces that may be applied to the flexure beam. Since, parallelogram and double parallelogram flexures are the most frequently used flexure units in this thesis, and since the beams that constitute these units have an approximately S-shape deformation, we shall use the S-shape deformation to make some preliminary estimates.

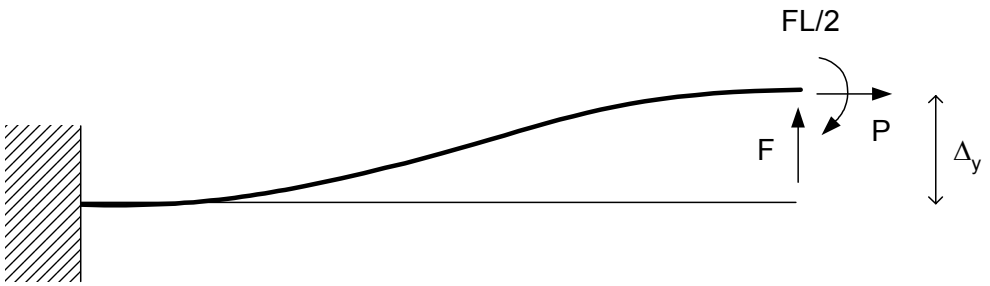

Fig 3.2 A beam deformed in S-shape

A beam experiences an S-shape deformation for the loading conditions shown in Fig 3.2. For this zero end slope condition, it can be shown that the buckling load of the beam is given by

$$P = -\frac{\pi^2 EI}{L^2} \Rightarrow \frac{PL^2}{EI} = -\pi^2 \approx -9.87$$

where all the quantities have standard meanings. As part of a parallel kinematic flexure the beam will transmit tensile as well as compressive loads. Hence we shall only be interested in axial loads that are within the buckling limit. Furthermore, the flexure units will transmit axial as well as transverse loads.

For a symmetric and balanced mechanism, the order of these loads will be approximately the same. Therefore, we shall use the limit determined above for the transverse loads F as well.
Using the maximum shear stress yield criteria, for example, one can show that the maximum allowable tip displacement is given by

$$\left(\frac{\Delta_y}{L}\right)_{\max} \leq \frac{1}{3\eta}\frac{S_y}{E}\frac{L}{T} \tag{3.2}$$

where T denotes the beam thickness, S_y is the material yield strength, and η is a chosen factor of safety. For flexures, L/T ratios of *50* are common, and S_y/E ratios range from *4e-3* for AL-6061 to *1e-2* for TI-13. The safety factor η may be chosen on the basis of stress concentration in the geometry. For typical values, the maximum deformation Δ_y ranges from *0.05L* to *0.1L*. We will aim to obtain results for deformations as large as *0.1L*, but in practice the deformations are kept well within this number, especially if fatigue loading is considered.

Based on (3.2), it is useful to keep in mind that in designs where the maximum motion is dictated by the static yield criteria, the normalized maximum motion Δ_y/L is inversely proportional to the normalized blade thickness T/L.

Now consider a Bernoulli beam in Fig. 3.3 with a set of generalized forces F, M and P acting at its tip, representing transverse, moment and axial loads, respectively. The resulting displacements are Δ_x, Δ_y and θ. All forces and displacements are expressed in a reference frame that is aligned with the undeformed configuration of the beam. The constitutive relation for an X differential element of the beam is given by Euler's formula (3.1). The macroscopic geometric compatibility can be stated as an expression for the beam curvature at any given location X along the beam length.

$$\frac{1}{\rho} = \frac{Y''}{(1+Y'^2)^{3/2}} \tag{3.3}$$

The denominator in the above term makes the resulting differential equation non-linear, and requires the use of elliptical integrals for a closed-form solution [73-75]. The result of this non-linear formulation is too complex to be of use for the closed-form analysis of more complex flexure mechanisms. Instead of trying to work with the elliptical integrals, we consider the often made assumption of small slopes. For an S-shape deformation if the tip deflection is *0.1L*, then the maximum slope that exists in the beam is *0.15*, which occurs at the mid-length. Therefore, the maximum error in approximating the denominator by *1* is about *3.4* percent. To meet the objective of obtaining parametric results, we decide to accommodate this error.

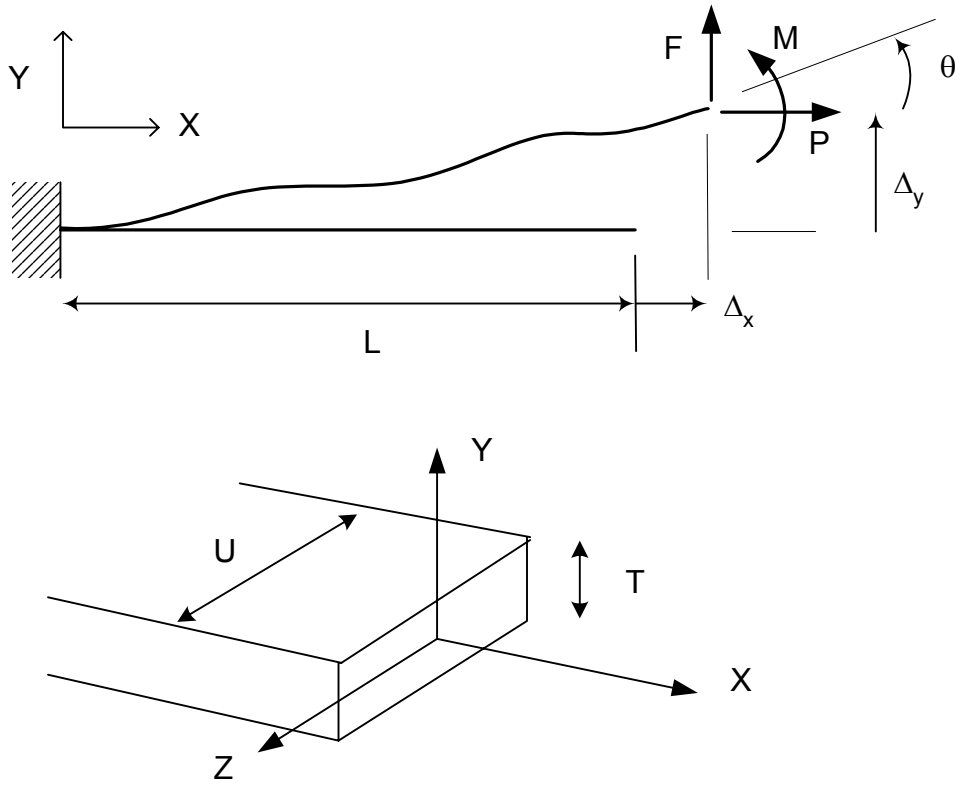

Fig 3.3 Beam with a generalized end load

In the next step, all displacements and length parameters are normalized by the beam length L, and all forces are normalized by EI/L^2.

$$y=\frac{Y}{L} \qquad x=\frac{X}{L} \qquad \delta_y=\frac{\Delta_y}{L} \qquad \delta_x=\frac{\Delta_x}{L} \qquad t=\frac{T}{L} \qquad u=\frac{U}{L}$$

$$m=\frac{ML}{EI} \qquad f=\frac{FL^2}{EI} \qquad p=\frac{PL^2}{EI}$$

In the rest of this thesis, we follow the notation of representing all non-dimensionalized quantities by lower case alphabets, whereas their corresponding dimensional parameters are denoted in upper case.

The condition of force equilibrium when determined from the undeformed configuration results in,

$$M(X)=M+F(L-X)\Rightarrow m(x)=m+f(1-x) \tag{3.4}$$

Equations (3.1)-(3.4) can be solved simultaneously to determine displacements in terms of loads or vice-versa. The results of this straightforward exercise are stated in a non-dimensionalized form.

$$\begin{bmatrix}\delta_y \\ \theta\end{bmatrix} = \begin{bmatrix}1/3 & 1/2 \\ 1/2 & 1\end{bmatrix}\begin{bmatrix}f \\ m\end{bmatrix}$$
$$\begin{bmatrix}f \\ m\end{bmatrix} = \begin{bmatrix}12 & -6 \\ -6 & 4\end{bmatrix}\begin{bmatrix}\delta_y \\ \theta\end{bmatrix} \tag{3.5}$$

$$\begin{aligned}\delta_x &= -\begin{bmatrix}\delta_y & \theta\end{bmatrix}\begin{bmatrix}3/5 & -1/20 \\ -1/20 & 1/15\end{bmatrix}\begin{bmatrix}\delta_y \\ \theta\end{bmatrix} + \frac{pt^2}{12} \\ &= -\begin{bmatrix}f & m\end{bmatrix}\begin{bmatrix}1/15 & 5/48 \\ 5/48 & 1/6\end{bmatrix}\begin{bmatrix}f \\ m\end{bmatrix} + \frac{pt^2}{12}\end{aligned} \tag{3.6}$$

Expression (3.6) is obtained by carrying out an integral of the beam arc length, and setting it equal to the undeformed length plus the elastic stretch. The resulting expression for δ_x is comprised of two very independent components, a kinematic term and an elastic term. While the elastic term depends on the applied axial force, and vanishes when the axial force becomes zero, the kinematic term has a quadratic dependence on the transverse displacements. Although the kinematic term expression may be rewritten in terms of transverse loads instead of transverse displacements, resulting in a non-linear force displacement characteristic, it is emphasized that this is fundamentally a relationship between geometric parameters, arising from the condition of geometric constraint on the arc length.

Note that the non-dimensionalized axial force *p* does not appear in the force-displacement relationships in the transverse directions (3.5). Furthermore, the relations (3.6) does not provide any information about the change in the axial stiffness in the presence of a transverse force or displacements. Such interdependence is of key concern in designing parallel kinematic mechanisms, as has been explained earlier. This linear analysis is good for displacements of the order of *0.1*, as long the axial force *p*, which was neglected in the force equilibrium relation, is small. The obvious questions that arise are: How small should *p* be for the expressions (3.5) and (3.6) to be effective? How are δ_y and θ affected by the presence of an axial load *p*? To obtain answers to these questions, we next perform a non-linear beam bending analysis based on force equilibrium conditions applied in the deformed configuration.

$$M(X) = M + F(L + \Delta_x - X) - P(\Delta_y - Y) \tag{3.7}$$

Equations(3.1), (3.3) and (3.7) together yield

$$EIY'' = M + F(L + \Delta_x - X) - P(\Delta_y - Y) \Rightarrow y'' = m + f(1 + \delta_x - x) - p(\delta_y - y)$$

which upon double differentiation leads to

$$y^{iv} = py'' \Rightarrow y^{iv} - k^2 y'' = 0\ , \qquad p \triangleq k^2 \tag{3.8}$$

p may be positive or negative, resulting in a real or imaginary k, respectively. Both these situations are easily dealt with. The general solution to this equation is,

$$y = c_1 e^{kx} + c_2 e^{-kx} + c_3 x + c_4$$

Constants c_1 through c_4 can be determined using the boundary conditions. Depending on whether we want to obtain forces in terms of displacements or displacements in terms of forces, we can use either of two sets of boundary conditions

Set A		or	Set B	
$y = 0$	$@\, x = 0$		$y = 0$	$@\, x = 0$
$y' = 0$	$@\, x = 0$		$y' = 0$	$@\, x = 0$
$y'' = m$	$@\, x = 1$		$y = \delta_y$	$@\, x = 1$
$y''' = -f + py'$	$@\, x = 1$		$y' = \tan\theta$	$@\, x=1$

At this point, we introduce two other approximations. $\tan\theta$ can be approximated by θ, since for the maximum slope of *0.15* that the beam sees, θ value is *0.149*, which is less than *1* percent error. Furthermore, although the boundary conditions should be applied in the deformed configuration, that is, at $x = 1 + \delta_x$, this is of very small consequence for the pertinent calculation. In an S shape deflection, for a δ_y of *0.1*, δ_x will be approximately *0.006*, which can be dropped out in comparison to *1* in the above boundary conditions.

Using the first set of boundary conditions, we obtain

$$c_1 = \frac{1}{e^k + e^{-k}} \left\{ \frac{m}{k^2} - \frac{f\ e^{-k}}{k^3} \right\}$$

$$c_2 = \frac{1}{e^k + e^{-k}} \left\{ \frac{m}{k^2} + \frac{f\ e^{k}}{k^3} \right\}$$

$$c_3 = f / k^2 \quad \text{and} \quad c_4 = -c_1 - c_2$$

With these values and some amount of mathematical manipulation, the end displacement of the beam can be shown to be,

$$\delta_y = f\left(\frac{k - \tanh k}{k^3} \right) + m\left(\frac{\cosh k - 1}{k^2 \cosh k} \right)$$

$$\theta = f\left(\frac{\cosh k - 1}{k^2 \cosh k} \right) + m\left(\frac{\tanh k}{k} \right) \tag{3.9}$$

If one employed the second set of boundary conditions, the values for the constants c_1 through c_4 are,

$$c_1 = \frac{k(e^{-k}-1)\Delta_y + (e^{-k}+k-1)\theta}{k\left[k(e^k-e^{-k})-2(e^k+e^{-k})+4\right]}$$

$$c_2 = \frac{k(e^{k}-1)\Delta_y - (e^{k}-k-1)\theta}{k\left[k(e^k-e^{-k})-2(e^k+e^{-k})+4\right]}$$

$$c_3 = k(c_2 - c_1)$$

$$c_4 = -c_1 - c_2$$

Given the following relationships for end loads,

$$f = -y'''(1) + py'(1)$$

$$m = y''(1)$$

one can deduce,

$$f = \frac{k^3 \sinh k}{k\sinh k - 2\cosh k + 2}\delta_y + \frac{k^2(1-\cosh k)}{k\sinh k - 2\cosh k + 2}\theta$$

$$m = \frac{k^2(1-\cosh k)}{k\sinh k - 2\cosh k + 2}\delta_y + \frac{k^2\cosh k - k\sinh k}{k\sinh k - 2\cosh k + 2}\theta \qquad (3.10)$$

Expressions analogous to (3.9) and (3.10) may be obtained similarly for compressive axial load, i.e., negative values of p. The results are obtained in terms of trigonometric functions rather than hyperbolic functions.

The next step in this derivation is to apply the constraint condition on the arc length of the beam in its deformed configuration, so as to determine δ_x . As earlier, the displacement δ_x can be resolved into two components – a kinematic component that results from the constant arc length requirement, and a purely elastic component that results due to elastic stretching.

$$\delta_x = \delta_x^k + \delta_x^e \qquad (3.11)$$

The elastic component may be expressed as,

$$\delta_x^e = \frac{p}{d} \qquad \text{where} \qquad d = \frac{AL^2}{I} = 12\left(\frac{L}{T}\right)^2 = \frac{12}{t^2} \qquad (3.12)$$

The kinematic component is derived by performing an integration on differential arc elements.

$$ds = (1+y'^2)^{1/2}dx \approx (1+\tfrac{1}{2}y'^2)dx$$

Clearly, in the above expression, we cannot simply neglect the *y'* term as was done earlier, or else we shall not be able to obtain a difference between the integral of *ds* and *dx*. We do however make a different assumption this time, by retaining up to the second order term in the Binomial expansion of the *ds* expression. The subsequent term is fourth order and for a maximum *y'* of *0.15*, this term is approximately *5e-4*, and is therefore neglected.

$$\int_0^{1+\delta_x^e} ds = \int_0^{1+\delta_x^e} (1 + \tfrac{1}{2} y'^2)\,dx$$

$$1 + \delta_x^e = (1 + \delta_x) + \tfrac{1}{2}\int_0^{1+\delta_x} y'^2\,dx \quad \Rightarrow \quad \delta_x^k = -\tfrac{1}{2}\int_0^{1} y'^2\,dx$$

We also note that the upper limit of integration has been changed in the last integral expression, on the basis that the small difference in the integral limit will not change the integral significantly. The length term appears in the integral appear in powers of three and higher, and since δ_x is approximately *0.006* for a maximum tip displacement of *0.1* for a beam in an S-shape deflection, it reasonable to neglect the δ_x with respect to the *1* that appears in the integral limit.

For the sake of mathematical convenience, this time we use an alternate expression for *y,* in terms of hyperbolic functions instead of exponentials. For this solution to be valid, we have to explicitly assume that the axial force is tensile. For compressive loads an analogous analysis can be conducted.

$$y = c_1 \cosh kx + c_2 \sinh kx + c_3 x + c_4$$
$$y' = c_1\ k \sinh kx + c_2\ k \cosh kx + c_3$$

Applying the boundary conditions,

$$@\,x = 0 \qquad\qquad @\,x = 1$$
$$y = 0 \Rightarrow c_1 + c_4 = 0 \qquad\qquad y = \Delta_y \Rightarrow c_1 \cosh k + c_2 \sinh k + c_3 + c_4 = 0$$
$$y' = 0 \Rightarrow c_2 k + c_3 = 0 \qquad\qquad y' = \theta \Rightarrow c_1 k \sinh k + c_2 k \cosh k + c_3 = 0$$

one may solve for the unknown constants in the solution, and subsequently for *y'*.

$$\begin{bmatrix} c_1 \\ c_2 \end{bmatrix} = \frac{1}{k \sinh k - 2\cosh k + 2} \begin{bmatrix} \cosh k - 1 & \dfrac{k - \sinh k}{k} \\ -\sinh k & \dfrac{\cosh k - 1}{k} \end{bmatrix} \begin{bmatrix} \Delta_y \\ \theta \end{bmatrix}$$

$$c_3 = -c_2 k$$
$$c_4 = -c_1$$

$$y' = c_1\ k\sinh kx + c_2\ k(\cosh kx - 1)$$

$$y'^2 = k^2 \begin{bmatrix} c_1 & c_2 \end{bmatrix} \begin{bmatrix} \sinh^2 kx & \sinh kx\ (\cosh kx - 1) \\ \sinh kx\ (\cosh kx - 1) & (\cosh kx - 1)^2 \end{bmatrix} \begin{bmatrix} c_1 \\ c_2 \end{bmatrix}$$

$$\int_0^1 y'^2 dx = k^2 \begin{bmatrix} c_1 & c_2 \end{bmatrix} \begin{bmatrix} \int_0^1 \sinh^2 kx\ dx & \int_0^1 \sinh kx\ (\cosh kx - 1)\ dx \\ \int_0^1 \sinh kx\ (\cosh kx - 1)\ dx & \int_0^1 (\cosh kx - 1)^2 dx \end{bmatrix} \begin{bmatrix} c_1 \\ c_2 \end{bmatrix}$$

$$= \frac{k}{2} \begin{bmatrix} c_1 & c_2 \end{bmatrix} \begin{bmatrix} (\cosh k \sinh k - k) & (\cosh^2 k - 2\cosh k + 1) \\ (\cosh^2 k - 2\cosh k + 1) & (\cosh k \sinh k - 4\sinh k + 3k) \end{bmatrix} \begin{bmatrix} c_1 \\ c_2 \end{bmatrix}$$

Ultimately, one can obtain

$$\delta_x^k = -\begin{bmatrix} \delta_y & \theta \end{bmatrix} \begin{bmatrix} r_{11} & r_{12} \\ r_{21} & r_{22} \end{bmatrix} \begin{bmatrix} \delta_y \\ \theta \end{bmatrix} \tag{3.13}$$

where,

$$r_{11} = \frac{k^2(\cosh^2 k + \cosh k - 2) - 3\sinh k(\cosh k - 1)}{2\left(k\sinh k - 2\cosh k + 2\right)^2}$$

$$r_{12} = r_{21} = -\frac{k^2(\cosh k - 1) + k\ \sinh k\ (\cosh k - 1) - 4(\cosh k - 1)^2}{4\left(k\sinh k - 2\cosh k + 2\right)^2}$$

$$r_{22} = \frac{-k^3 + k^2 \sinh k(\cosh k + 2) - 2k\ (2\cosh^2 k - \cosh k - 1)\ + 2\sinh k\ (\cosh k - 1)}{4k\left(k\sinh k - 2\cosh k + 2\right)^2}$$

As earlier, δ_x^k may be stated in terms of the transverse loads instead of displacements, but it should be recognized that this is fundamentally an equation of geometric constraint – that the beam maintains a constant arc length. It may be may be noticed that this condition of geometric constraint is explicitly dependent on a load in the form of *k*. As indicated earlier, such situations are fairly uncommon. It will be shortly seen that this load dependence is very weak, nevertheless, it existence is of much importance.

The final results of this derivation are the five equations (3.9)-(3.13) relating five displacement variables - θ, δ_y, δ_x, δ_x^k, δ_x^e, and three load terms *f*, *m*, and *p*. The last three equations may be combined to result in an overall three equations, and six variables. Given any three, the remaining three can be found. These results match with similar analysis that has been done in the past [76].

Based on the approximations made so far, these results should err by no more 3-4 % in predicting the true behavior of an ideal beam. It is noteworthy that in the above analysis, we have ignored the non-linearity in the geometric compatibility conditions but have incorporated the non-linearity from the force equilibrium equation. This judgment is based on the fact that, while the former approximation results in a few percent error in the displacement estimates, ignoring the non-linearities in the force equilibrium results in the loss of some fundamental physical effects that dictate the performance of flexures. Furthermore, it will be seen in the next section that the transcendental expressions (3.9) and (3.10), resulting from the force equilibrium non-linearity, can be readily simplified to obtain useful parametric information. Similar simplifications are difficult to obtain for elliptical integrals.

3.2 Engineering Approximations and Simplified Results

Several interesting observations can be made from the expressions stated above. For example, the end displacements y and θ are not uniquely related to the end loads f and m. For any given loads, f and m, the displacements, y and θ, can take a different set of values depending on the magnitude of k, or the axial load p. But given the transcendental nature of the above expressions, it is almost impossible for a design engineer to draw any parametric conclusions. We therefore proceed to make another set of engineering approximations, the most important so far, in an attempt to obtain expressions that offer better insight into the force displacement characteristics of the flexure beam.

We start with the simplification of the compliance terms in Equation (3.9). An obvious first guess to expand the hyperbolic expression in form of an infinite series and then use the first few terms.

$$C = \begin{bmatrix} \left(\frac{k-\tanh k}{k^3}\right) & \left(\frac{\cosh k - 1}{k^2 \cosh k}\right) \\ \left(\frac{\cosh k - 1}{k^2 \cosh k}\right) & \left(\frac{\tanh k}{k}\right) \end{bmatrix}$$

$$c_{11} = \left(\frac{k-\tanh k}{k^3}\right) \approx \frac{1}{3}\left(1 - \frac{2}{5}k^2 + \frac{17}{105}k^4 - \frac{62}{945}k^6 \ldots\right)$$

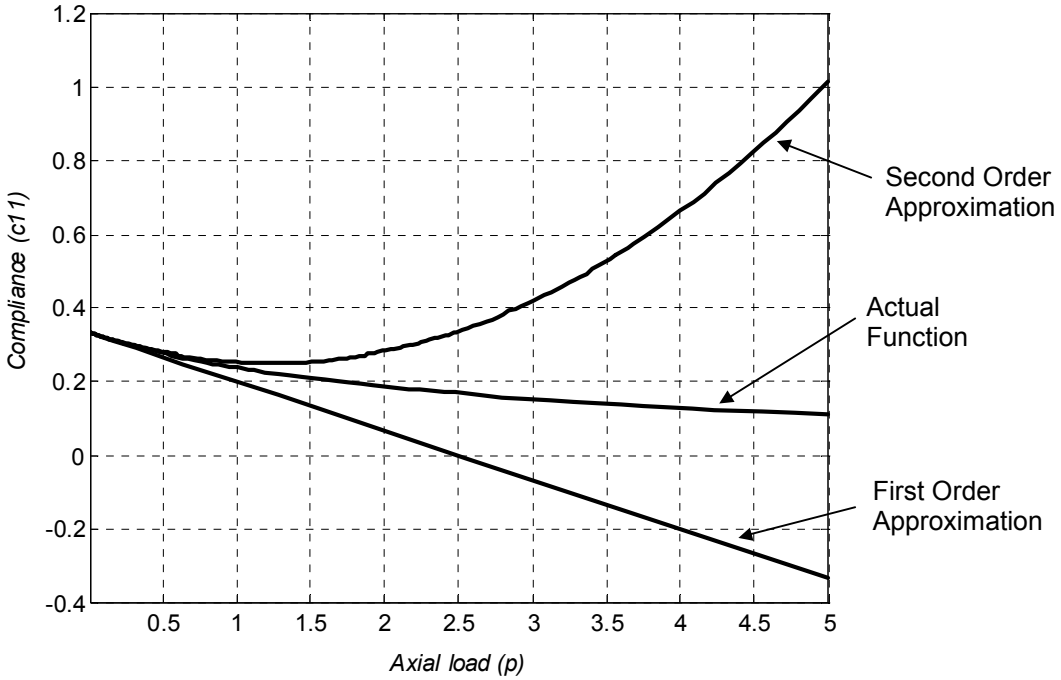

Fig 3.4 Approximation of the Compliance term c_{11}

Simply taking the first few terms from the expansion series turns out to be a very poor approximation as is seen in the Fig. 3.4. Instead we look for other simple functions that may approximate the transcendental function. The following turns out be a good fit.

$$\left(\frac{k-\tanh k}{k^3}\right) \approx \frac{1}{3}\left(1-0.4k^2+0.1619k^4-0.0656k^6\ldots\right)$$

$$\frac{1}{3(1+\frac{2}{5}k^2)} \approx \frac{1}{3}\left(1-0.4k^2+0.1600k^4-0.0640k^6\ldots\right)$$

Since the series expansion coefficients for the two functions are very close up to several higher order terms, the expression in the second line above seems to be a very good approximation. This becomes evident from Fig.3.5 where the two functions are plotted for values of p ($\triangleq k^2$) up to *10*. At this value of *p*, the error in approximation is 2.6%. Mathematically speaking, this excellent match is purely a coincidence.

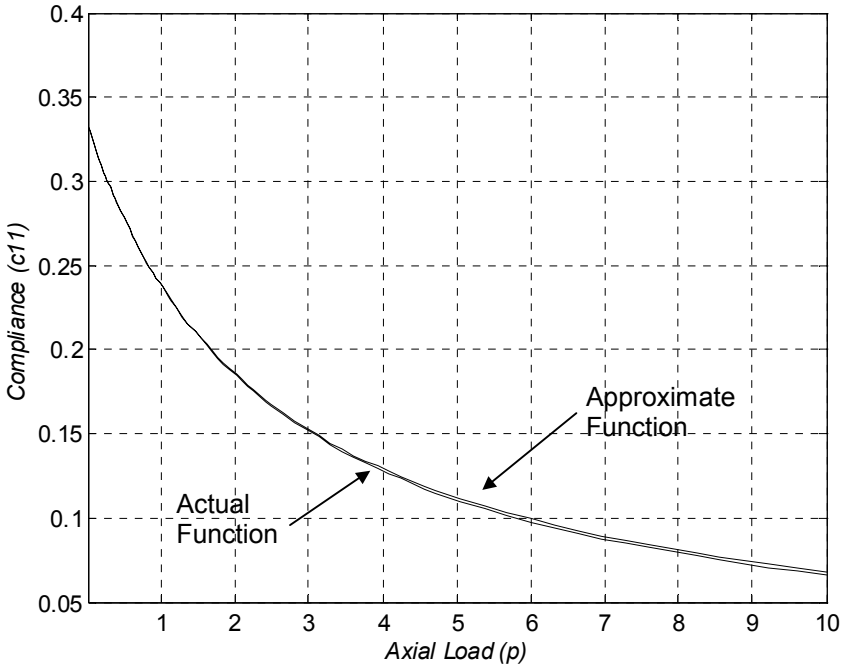

Fig 3.5 Approximation of the Compliance term c_{11}

Similar approximations may be obtained for the other compliance terms.

$$c_{12} = c_{21} = \left(\frac{\cosh k - 1}{k^2 \cosh k} \right) \approx \frac{1}{2\left(1 + \frac{5}{12} k^2\right)} = \frac{1}{2\left(1 + \frac{5}{12} p\right)}$$

$$c_{22} = \left(\frac{\tanh k}{k} \right) \approx \frac{1}{\left(1 + \frac{1}{3} k^2 - \frac{1}{63} k^4\right)} = \frac{1}{\left(1 + \frac{1}{3} p - \frac{1}{63} p^2\right)}$$

$$c_{22} = \left(\frac{\tanh k}{k} \right) \approx \frac{\left(1 + \frac{1}{10} p\right)}{\left(1 + \frac{17}{40} p + \frac{7}{600} p^2\right)}$$

These approximate functions are plotted in Figures 3.6 and 3.7 respectively, along with the exact functions. Since these are not series based approximations, p does not have to be small for the approximations to hold. While the approximation for c_{11} and c_{12} is good for values of p up to *10*, the approximation for c_{22} is not as accurate. In fact, simply an inverse linear term results in an inadequate match in this case, and therefore a quadratic term is also included, which improves the approximation for values of p up to *5*. A combination of linear and inverse quadratic function, shown above, may also be used to get an even better approximation.

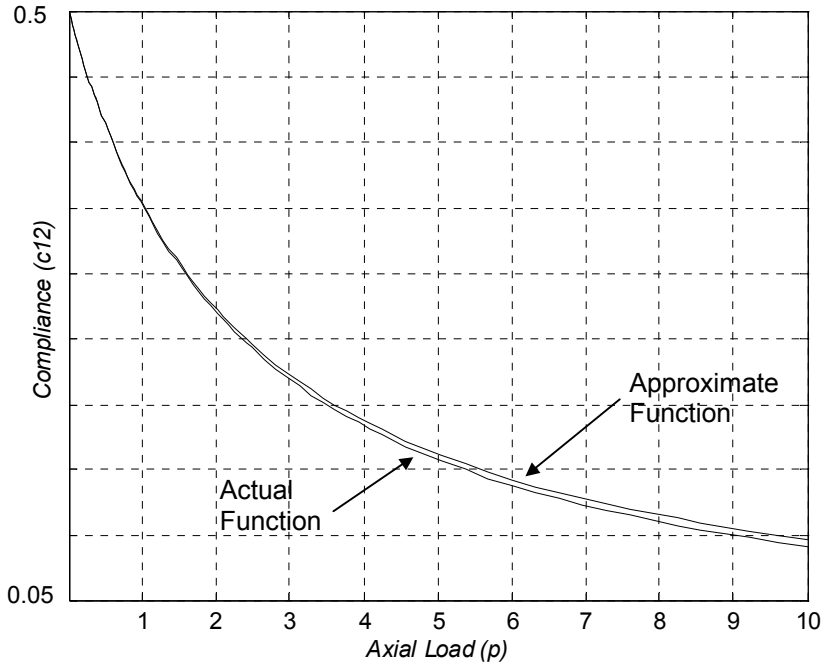

Fig 3.6 Approximation of the Compliance term c_{12}

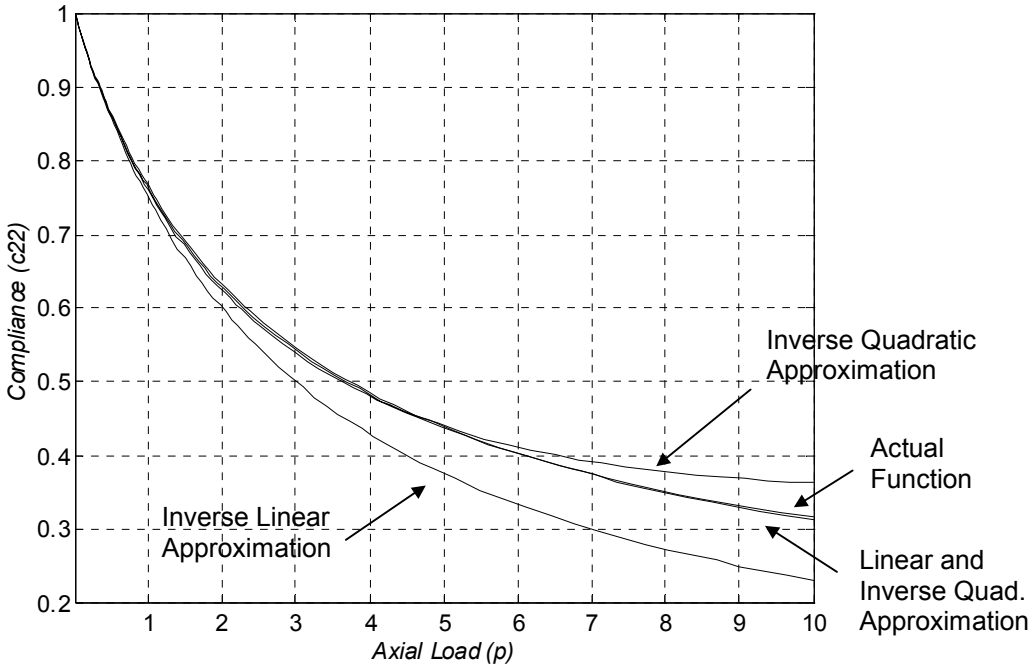

Fig 3.7 Approximation of the Compliance term c_{22}

The fact that some compliance terms can be approximated by inverse linear functions of p, provides an indication that stiffness functions may be approximated by linear functions of p. That indeed is the case, and therefore approximations to the stiffness terms are obtained simply from the Taylor series expansion of the actual hyperbolic stiffness functions.

$$K = \begin{bmatrix} \dfrac{k^3 \sinh k}{k\sinh k - 2\cosh k + 2} & \dfrac{k^2(1-\cosh k)}{k\sinh k - 2\cosh k + 2} \\ \dfrac{k^2(1-\cosh k)}{k\sinh k - 2\cosh k + 2} & \dfrac{k^2\cosh k - k\sinh k}{k\sinh k - 2\cosh k + 2} \end{bmatrix}$$

The following series expansions show that for the range of our interest, the coefficients of the higher order terms are small enough to be neglected.

$$k_{11} = \frac{k^3 \sinh k}{k\sinh k - 2\cosh k + 2} \approx 12\left(1 + \tfrac{1}{10}k^2 - \tfrac{1}{8400}k^4 \ldots\right) \approx 12\left(1 + \tfrac{1}{10}p\right)$$

$$k_{12} = \frac{k^2(1-\cosh k)}{k\sinh k - 2\cosh k + 2} \approx -6\left(1 + \tfrac{1}{60}k^2 - \tfrac{1}{8400}k^4 \ldots\right) \approx -6\left(1 + \tfrac{1}{60}p\right)$$

$$k_{22} = \frac{k^2\cosh k - k\sinh k}{k\sinh k - 2\cosh k + 2} \approx 4\left(1 + \tfrac{1}{30}k^2 - \tfrac{11}{25200}k^4 \ldots\right) \approx 4\left(1 + \tfrac{1}{30}p\right)$$

The first two simplifications above result in errors of less than *1* percent, and the third simplification deviates from the exact expression by less than *3* percent. But the advantage of these simplifications are far-fetched in terms of revealing the key attributes of the beam flexure, and producing valuable closed-form results. Although the above approximations are obtained for tensile axial loads, the approximations can be shown to be valid for compressive axial loads as well. It can also be shown that the product of the approximate stiffness matrix and the approximate compliance matrix, both restated below, is very close to the unity matrix.

$$\begin{bmatrix} \delta_y \\ \theta \end{bmatrix} = \begin{bmatrix} \dfrac{1}{3\left(1 + \frac{2}{5}p\right)} & \dfrac{1}{2\left(1 + \frac{5}{12}p\right)} \\ \dfrac{1}{2\left(1 + \frac{5}{12}p\right)} & \dfrac{\left(1 + \frac{1}{10}p\right)}{\left(1 + \frac{17}{40}p + \frac{7}{600}p^2\right)} \end{bmatrix} \begin{bmatrix} f \\ m \end{bmatrix} \tag{3.14}$$

$$\begin{bmatrix} f \\ m \end{bmatrix} = \begin{bmatrix} 12\left(1 + \frac{1}{10}p\right) & -6\left(1 + \frac{1}{60}p\right) \\ -6\left(1 + \frac{1}{60}p\right) & 4\left(1 + \frac{1}{30}p\right) \end{bmatrix} \begin{bmatrix} \delta_y \\ \theta \end{bmatrix} \tag{3.15}$$

Luckily, simple linear approximations are also available for the coefficients in the geometric constraint relation (3.13). It may be seen that the coefficients have an approximately linear dependence on p, and that this dependence is very weak.

$$\delta_x^k = -\begin{bmatrix}\delta_y & \theta\end{bmatrix}\begin{bmatrix}\frac{3}{5}\left(1-\frac{p}{420}\right) & -\frac{1}{20}\left(1-\frac{p}{70}\right)\\ -\frac{1}{20}\left(1-\frac{p}{70}\right) & \frac{1}{15}\left(1-\frac{11p}{420}\right)\end{bmatrix}\begin{bmatrix}\delta_y\\ \theta\end{bmatrix} \tag{3.16}$$

It is therefore tempting to neglect the dependence of the coefficients on the axial loads. But it shall soon become clear that that these terms play a critical role in determining the characteristics of the beam in particular, and flexures in general.

Based on the recent approximations, the force-displacement relations for a blade can be stated as follows.

$$\begin{bmatrix}f\\ m\end{bmatrix} = \begin{bmatrix}a & c\\ c & b\end{bmatrix}\begin{bmatrix}\delta_y\\ \theta\end{bmatrix} + p\begin{bmatrix}e & h\\ h & g\end{bmatrix}\begin{bmatrix}\delta_y\\ \theta\end{bmatrix} \tag{3.17}$$

$$\delta_x = \frac{1}{d}p + \begin{bmatrix}\delta_y & \theta\end{bmatrix}\begin{bmatrix}i & k\\ k & j\end{bmatrix}\begin{bmatrix}\delta_y\\ \theta\end{bmatrix} + p\begin{bmatrix}\delta_y & \theta\end{bmatrix}\begin{bmatrix}r & q\\ q & s\end{bmatrix}\begin{bmatrix}\delta_y\\ \theta\end{bmatrix} \tag{3.18}$$

These are three equations and six unknowns – three loads and three displacements. Given any three, the remaining can now be easily solved analytically for most cases. The coefficients *a*, *b*, *c*, *d*, *e*, *g*, *h*, *i*, *j*, *k*, *q*, *r* and *s* are all non-dimensional numbers and are characteristic of the uniform cross-section thin beam.

a	12	*e*	1.2	*i*	-0.6	*r*	1/700
b	4	*g*	2/15	*j*	-1/15	*s*	11/6300
c	-6	*h*	-0.1	*K*	1/20	*q*	-1/1400

These numbers obviously remain unchanged as the size of the beam varies, but do change when the geometry or the shape of the beam changes. The variation in above coefficients with changes in beam geometry forms the basis for a sensitivity analysis which shall be briefly discussed later in this chapter.

3.3 Observations and Comments on the Simplified Results

There are many interesting observations that may be drawn from the above derivations, also several comments that can be made on these derivations.

1. We see that the transverse stiffness terms are approximately a linear function of the axial force. Although it is intuitively known that the transverse stiffness of a beam increases with a tensile axial load and decreases with a compressive axial load, the actual dependence is stated here in a quantitative form. The non-linearity in force displacement relationships arises due to the fact that displacements are included in force equilibrium. It is common to refer to two kinds of stiffness, the

elastic stiffness matrix and the geometric stiffness matrix, clearly distinguished in expression (3.17). Apart from playing an important role in the analysis of more complex mechanisms, these expressions may be used to quickly and symbolically obtain results that would otherwise involve tedious analysis. For example, in the presence of an axial load *p,* one can easily derive the ratio between *m* and *f*, that is needed to maintain a zero end slope, to be

$$\frac{m}{f} = -\frac{1}{2}\frac{\left(1+\frac{1}{60}p\right)}{\left(1+\frac{1}{10}p\right)}$$

Similarly, the non-linear *Duffing effect* in a clamped-clamped beam, transversely loaded in the middle, can be obtained in a few steps to be,

$$f = \left(a - i\ d\ e\ \delta_y^{\ 2}\right)\delta_y \tag{3.19}$$

2. Despite being based on several assumptions, these approximate results are accurate to within *5* percent of the real behavior of an ideal beam. This may be validated using known cases of beam buckling. One way of defining buckling is – the limit of compressive axial force when transverse stiffness becomes zero. For a fixed-free beam, applying the boundary condition of *m=0* in equation (3.14), one obtains $\delta_y = \frac{1}{3\left(1+\frac{2}{5}p\right)}f \ \Rightarrow\ p_{crit} = -2.5$. From the classical linear beam buckling analysis, the critical buckling load for a fixed free beam is known to be $P_{crit} = -\frac{\pi^2}{4}\frac{EI}{L^2}$ $\Rightarrow p_{crit} = -\frac{\pi^2}{4} = -2.4674$, which is about *1.3%* off from the value predicted using the approximate results. Similarly, one may consider the buckling of a beam that is fixed on one end, and is constrained to have a zero slope on the other end. This time we can make use of equation (3.15) to predict that the transverse stiffness of the beam will drop to zero for a compressive load of *p=10* , which is also *1.3%* off from the value π^2, derived from linear beam buckling. For obvious reasons, these results may not be used for predicting the buckling of pinned-pinned or clamped-clamped beams.

3. While the analysis in Section 3.2 assumed that the loads in the deformed configuration stay aligned with the undeformed reference axes of the flexure beam, other situations are easily addressed using the results of the above derivation. Consider, for example, the loading situation of Fig. 3.8, where the loads translate and rotate with the beam tip.

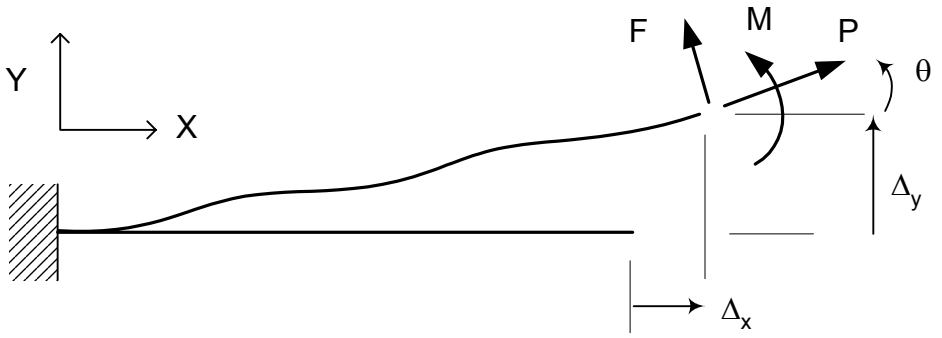

Fig 3.8 End loading that maintains the orientation of beam tip

Since θ represents rotation of beam tip and is not a spatial variable, this loading condition offers no significant problems, other than some added mathematical complexity. The tip loads expressed along the XY axes may be stated as,

$$f^* = f\cos\theta + p\sin\theta \approx f(1-\tfrac{1}{2}\theta^2) + p\theta$$
$$p^* = p\cos\theta - f\sin\theta \approx p(1-\tfrac{1}{2}\theta^2) - f\theta$$

Substituting these in equations (3.14) and (3.15) yields interesting force displacement relationships. For the particular case of $p=0$ and $m=0$, it can be shown in a few steps that

$$\frac{\theta}{(1+\tfrac{1}{3}\theta^2)} = \frac{f}{2} \qquad \text{and} \qquad \delta_y \approx \frac{f-\tfrac{1}{8}f^3}{3-\tfrac{3}{5}f^2}$$

As expected, the transverse stiffness reduces as a consequence of this loading condition.

4. While the variation of transverse stiffness due to axial loads is very clear from equation (3.17), the change in axial stiffness due to the presence of a transverse displacement is quantified in equation (3.18). It may be seen that the kinematic component defined earlier may be further separated into a purely kinematic component, and an 'elastokinematic' component.

$$\delta_x^e = \frac{1}{d}p \qquad \delta_x^k = \begin{bmatrix}\Delta_y & \theta\end{bmatrix}\begin{bmatrix} i & k \\ k & j\end{bmatrix}\begin{bmatrix}\delta_y \\ \theta\end{bmatrix} \qquad \delta_x^{ek} = p\begin{bmatrix}\Delta_y & \theta\end{bmatrix}\begin{bmatrix} r & q \\ q & s\end{bmatrix}\begin{bmatrix}\delta_y \\ \theta\end{bmatrix}$$

The first term above represents a purely elastic component that results from stretching of the beam. The second term is a purely kinematic component, and is a consequence of the constant beam arc length requirement. The third term is the most interesting of three because it has both an elastic as well as a kinematic aspect. Although this term is also a consequence of the constant beam arc length requirement, it essentially captures the effect of the change in the beam's deformed shape due to the

contribution of the axial force to the bending moments. The first and the third components contribute to the compliance in the X-direction, while the second component is independent of the axial force. The importance of the third term is due to its non-linear contribution to the axial compliance, which has a quadratic dependence on the transverse displacements. As has been mentioned earlier, the axial stiffness of a beam flexure determines the quality of its DOC, which in turn influences static as well as dynamic performance measures in a flexure mechanism.

5. Furthermore, a generalization of the above analysis for a uniform beam may be made by considering a different beam shape, for example, the common double notch flexure in Fig. 3.9.

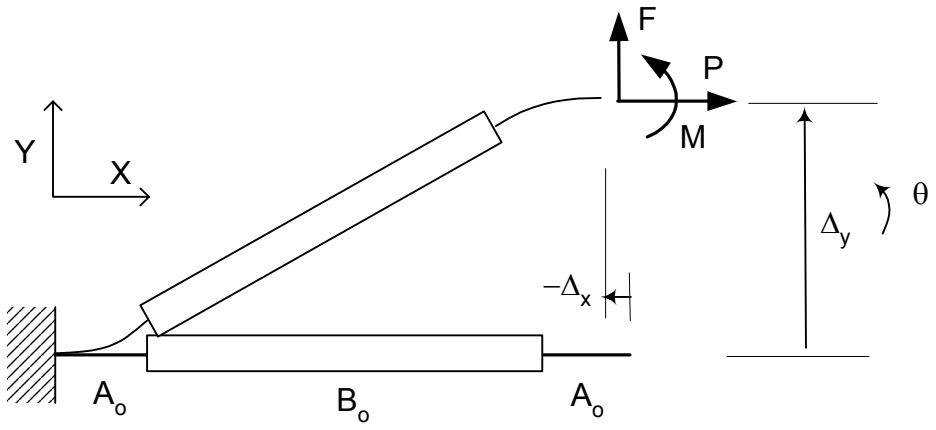

Fig. 3.9 Double Notch Flexure

The overall length of the beam is still L and is used as the characteristic length of the system. The two notches are A_o each, and the length of the rigid connector is B_o. Analysis analogous to that of Section 3.2 can be carried out, although this involves a bit more mathematical complexity. In general, the structure of resulting expressions remains the same, while the non-dimensional coefficients vary. The transverse force displacement relationships in the absence of the axial load *p* are given by

$$\begin{bmatrix} \delta_y \\ \theta \end{bmatrix} = \begin{bmatrix} \left(\frac{2}{3}a_o^{\,3} - a_o^{\,2} + a_o\right) & a_o \\ a_o & 2a_o \end{bmatrix} \begin{bmatrix} f \\ m \end{bmatrix}$$

$$\begin{bmatrix} f \\ m \end{bmatrix} = \begin{bmatrix} \frac{12}{1-b_o^{\,3}} & \frac{-6}{1-b_o^{\,3}} \\ \frac{-6}{1-b_o^{\,3}} & \frac{4+b_o+b_o^{\,2}}{1-b_o^{\,3}} \end{bmatrix} \begin{bmatrix} \delta_y \\ \theta \end{bmatrix}$$

These relations reduce to (3.14) and (3.15), if b_o is set to *0* or a_o is set to *0.5*, and *p=0*. Obviously, if a_o is made very small, Bernoulli's assumptions will start to fail, and a more accurate analysis will be

needed. Nevertheless, these results provide us with an idea of how the non-dimensional coefficients vary with changing geometry. As is expected, increasing the ratio b_o will increase the transverse stiffness since this reduces the a_o segments that provide compliance. For small values of b_o the stiffness matrix above can be approximated by

$$\begin{bmatrix} f \\ m \end{bmatrix} = \begin{bmatrix} 12(1+3b_o) & -6(1+3b_o) \\ -6(1+3b_o) & 4(1+3b_o) \end{bmatrix} \begin{bmatrix} \delta_y \\ \theta \end{bmatrix}$$

Interestingly, this is very similar to the effect that an axial load p has on transverse stiffness, as given by (3.15). In fact, even the deformations of the double notch flexure, and a beam flexure under a large axial load, are very similar. In the former case, the shape of the flexure is such that only the a_o segments bend and have a curvature, whereas the b_o segment, being rigid, obviously has no curvature. On the other hand, in the latter case, the effect of the axial force of the beam deformation is such that curvature is predominantly limited to beam ends, and the middle section of the beam remains relatively straight.

Furthermore, such a quantification of the effect of geometric shape variations of the beam on its force-displacement characteristics provides a perfect basis for shape synthesis or optimization, as discussed in Section 1.2. Other variations of the flexure unit in Fig. 3.9, for example, finite stiffness of the middle segment, may also be considered. Each such embodiment will produce a different set of non-dimensional coefficients, but the fundamental physical effects identified above will remain the same. For this reason, all the subsequent discussions on mobility and error motions is pertinent to flexure mechanisms based on a wide range of building blocks, and not simply the uniform beam.

3.4 Mobility of Flexure Mechanisms

Based on the understanding gained in the above analysis and subsequent simplifications, we are now in a position to discuss the concepts of Degrees of Freedom, Degrees of Constraint, and overconstraint in flexure mechanisms. A brief summary of the existing literature on mobility analysis of flexures mechanisms was presented in Chapter 1.

Before we proceed, it is worthwhile to first take a quick look at the DOF definition in the context of rigid-link mechanisms. In the case of rigid-link mechanisms, DOF is defined in several ways, the most fundamental of which is – the minimum number of independent displacement coordinates necessary to completely define the configuration of a mechanism. These displacement coordinates are a subset of the so called generalized coordinates, which exceed the DOF by the number of geometric constraints in the

system. This definition of DOF also translates to – the maximum number of independent displacement inputs that can be specified to a given mechanism without violating any geometric constraints. Externally applied loads do not play any role in the mobility of rigid-link mechanisms because the stiffness of constituent elements is either zero or infinite. As is obvious from these definitions, DOF is a purely kinematic property of rigid-link mechanisms, and remains the same for static as well as dynamic analysis.

Gruebler's criterion [24,77] is the most common method of determining the DOF of rigid-link mechanisms. This criterion is derived by considering the DOF of the various constituent rigid links, and the DOC of the elements that connect the rigid links. Since this derivation is based on a generalized geometry of constituent links and connections, Gruebler's criterion fails to correctly predict the mobility of mechanisms that have special geometric arrangements. Several two and three dimensional examples are available in the literature [77], and two cases are shown in Fig. 3.10.

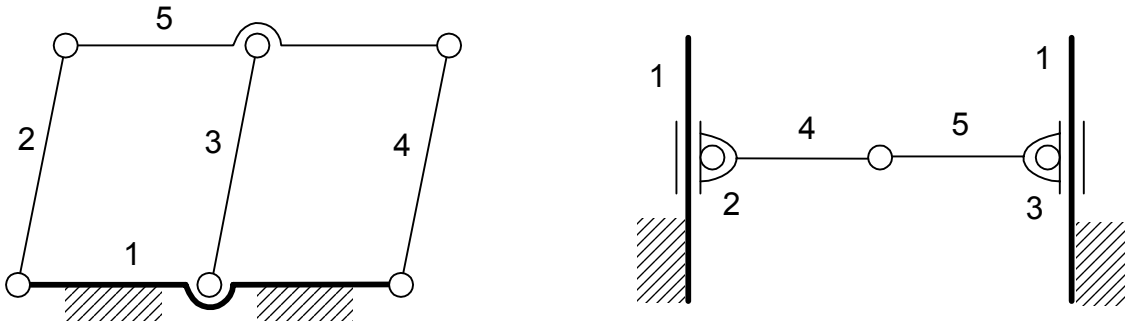

Fig. 3.10 Mechanisms for which Guebler's Criteria fails

Specifically, the method fails in situations where a particular geometric arrangement produces either redundant DOC or redundant DOF. For the first mechanism illustrated in Fig. 3.10, the DOF is predicted to be *0* for a general geometry, but for the particular case when links 2, 3 and 4 are perfectly parallel and equal in length, the constraint imposed by one of these three links and its associated pivots becomes redundant, making the actual DOF *1*. In the second mechanism, a general geometry will results in two DOF, but for the specific case when the sum of lengths of beams 4 and 5 is exactly equal to the distance between the two perfectly parallel guide rails, one of the DOF becomes redundant and the overall DOF is reduced to *1*.

This exposes a fundamental limitation of any mobility criterion that determines the DOF of a mechanism based on the DOF and DOC of its constituents. Because of its generality, which is a powerful as well as desirable attribute, any such criterion is unable to recognize any specific geometric configuration.

With this realization we now move on to flexure mechanisms. In somewhat loose terms, any stiff directions may be termed as Degrees of Constraint and compliant directions may be called Degrees of Freedom. But as soon as one defines DOF based on stiffness, it becomes necessary to specify the load and displacement that the stiffness is associated with.

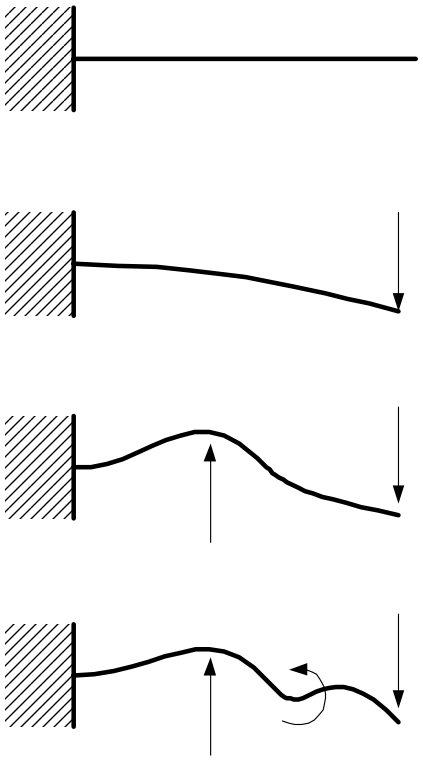

Fig. 3.11 Loads applied to an elastic body

It becomes obvious that, unlike rigid link mechanisms, applied loads have a role to play in determining the mobility in flexure mechanisms. In general, an infinite number of independent forces can be applied to an elastic body which result in infinite possible geometric configurations of the body, as shown in Fig. 3.11. With every new force that is added, the body takes a new shape, thereby requiring an ever-increasing number of independent coordinates to completely specify its geometry. To be able to talk about finite DOF in this context, one first needs to clearly identify all the possible locations on a given mechanism where generalized loads, three for a planer case and six for a general case, may be applied. The finite number of loads associated with these locations, or nodes, are referred to as the 'allowable loads' henceforth. The concept of introducing a real or imaginary node at locations where forces may be applied has been discussed in the literature [20-21]. This step is crucial as it allows one to associate a finite DOF with a compliant mechanism.

In this discussion we shall consider planer or two-dimensional cases only; an extension of these concepts to three dimensional mechanisms is analogous. Having identified the nodes where loads are allowed, we can associate three displacement coordinates with each. Although these displacement coordinates will be sufficient to determine the configuration of the entire mechanism, it remains to be determined which of these displacement coordinates contribute to Degrees of Freedom.

The extent of normalized displacements in response to nominal normalized loads, or simply the non-dimensional compliance, may be used as measure of mobility. For example, the maximum number of independently large displacement coordinates that can be obtained under any combination of the normalized allowable forces, each less than or equal to 1 unit in magnitude, can be defined as the DOF of the mechanism. If n is the number of nodes where forces may be applied, then the actual number of applied forces may be less than or equal to $3n$. The number of displacement coordinates will be equal to $3n$, and the DOF of the mechanism will be less than or equal to the number of applied loads. Note that the DOF doesn't have to be equal to either the number of applied loads or the total number of displacement coordinates. This is a robust definition for DOF and allows for the fact that a mechanism can have different DOF depending on the number of allowable loads.

Having obtained a clear definition of DOF in flexure mechanisms, the next step is to identify methods or criteria to determine it. Two possible approaches are considered here. The first approach is analogous to Gruebler's criterion, where the DOF of constituent flexure connections is predetermined using the above definition. The suggested exercise would in general be straightforward to perform on flexure units or building blocks. But as explained for the rigid-link mechanism case, any criterion that is based on the properties of the building blocks will be general and easy to apply, but will not account for special geometric configurations which can affect the mobility. Therefore, although simple, this may not always yield correct results. The alternate approach is to apply the above DOF definition to the entire mechanism without determining the DOF of the constituent flexure units. This becomes a case specific analysis, which gets more difficult with increasing complexity in the mechanism, but on the other hand is very reliable. Often, in the design flexure mechanisms, we consider cases with special geometric configurations to exploit the principles of reversal and symmetry. Due to the finite stiffness properties of flexures, they are more tolerant to underconstraint and overconstraint situations. In view of this, the second approach gains significance. The analytical tools presented earlier in this chapter help simplify the compliance estimates for the overall mechanism as required by this approach.

The entire discussion on DOF determination for flexure mechanisms has been based on large and small displacements in response to large and small forces. A non-dimensional analysis, as done in this chapter, is very helpful in this regard. To determine DOF of either a flexure unit or mechanism, a set of allowable

loads, each having a normalized magnitude of *1*, should be applied. Next, the normalized compliance of each displacement coordinate, considered one at a time, with respect to every allowable load should be computed. Compliance that is computed in this fashion includes the effects of nominal loads and displacements on the force-displacement characteristics of the mechanism. If the value of a normalized compliance for a certain displacement coordinate is of the order of 0.01 – 1.0, the coordinate is a potential candidate for a DOF, and if it is of the order of 0.01 or smaller, it becomes a DOC. Of the potential DOF candidates, the maximum number that can be independently set to be in the 0.01 – 1.0 range, in response to any combination of applied loads less than *1* in magnitude, will be the DOF. The normalized compliance values also provide an estimate of the relative quality of a Degree of Freedom or Constraint.

Let us consider the beam of Fig. 3.3 as an example, where forces are allowable at the beam tip. Therefore, there are three displacement coordinates: δ_x, δ_y and θ. From expressions (3.17) and (3.18), the normalized compliances associated with these displacement variables may be determined in the presence of unit normalized loads.

$$c_{11} = \frac{\partial \delta_y}{\partial f} = \frac{1}{3(1+0.4p)} = 0.283 \qquad c_{12} = \frac{\partial \delta_y}{\partial m} = \frac{1}{2\left(1+\frac{5}{12}p\right)} = 0.353 \qquad c_{13} = \frac{\partial \delta_y}{\partial p} = -0.376$$

$$c_{21} = \frac{\partial \theta}{\partial f} = \frac{1}{2\left(1+\frac{5}{12}p\right)} = 0.353 \quad c_{22} = \frac{\partial \theta}{\partial m} = \frac{\left(1+\frac{1}{10}p\right)}{\left(1+\frac{17}{40}p+\frac{7}{600}p^2\right)} = 0.7657 \quad c_{23} = \frac{\partial \theta}{\partial p} = -0.273$$

$$c_{33} = \frac{\partial \delta_x}{\partial p} = \frac{1}{d} + \begin{bmatrix} \delta_y & \theta \end{bmatrix} \begin{bmatrix} r & q \\ q & s \end{bmatrix} \begin{bmatrix} \delta_y \\ \theta \end{bmatrix}$$

Clearly, the first two displacement coordinates are large, and are potential candidates for DOF. Compliance of δ_x with respect to all the three allowable forces is seen to be very low over nominal ranges of motion, and therefore this displacement coordinate qualifies as a DOC. If suppose only a transverse force were allowed at the beam tip, even though the compliance associated with both δ_y and θ would have been high, but the DOF would be 1 since the two displacements cannot be varied independently with the single allowable force *f*. The deterioration of the quality of DOF with increasing axial loads is evident in the first two sets of expressions above and the deterioration in the quality of DOC in the X direction with displacements in the transverse directions is evident from expression for c_{33}. Thus, the analysis of Section 3.1 allows one to gauge the change in quality of Degrees of Freedom and Constraints in a flexure mechanism as forces and displacements vary.

Several other flexure units or mechanisms may be similarly considered, and the effectiveness of the definition of mobility provided here can be verified. One particular example is considered in Fig. 3.12 to illustrate a case of overconstraint.

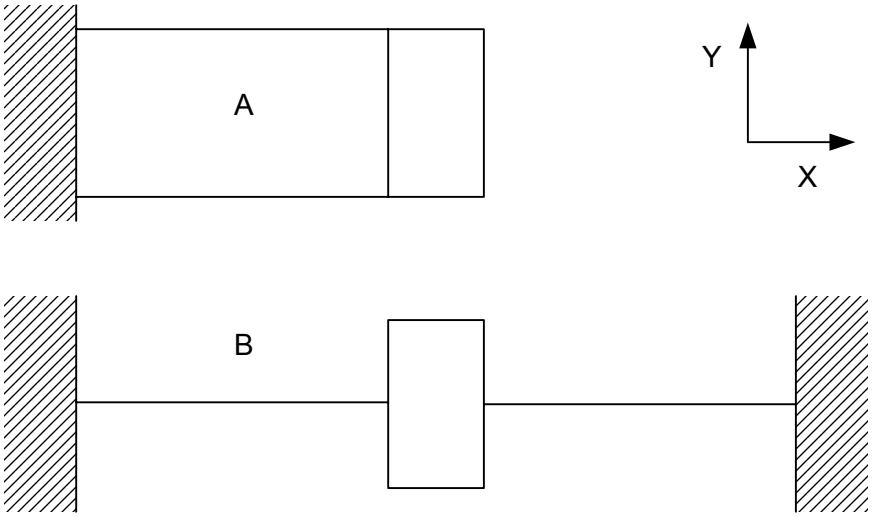

Fig. 3.12

The two cases considered in Fig. 3.12 are topologically identical. We have already shown that the DOF for the beam flexure unit given a general force at the tip is 2. Using the Gruebler's criterion, the DOF for the both the mechanisms should be 1. But we know from experience that this result is true for Mechanism A, but it is not entirely true for Mechanism B. We therefore resort to the latter approach explained earlier, where instead of relying on the DOF of the constituent units, the DOF of the mechanism is determined directly. In this case, the compliance in the Y direction can be determined from expression (3.19). It may be seen that the compliance is large (~ *0.026*) for small displacements of the order of t and starts decreasing quadratically as the displacements are increased (~ *4e-4* , for $\delta_y \sim 10t$) . Based on this, it is can be recognized that the Y displacement coordinate in Fig. 3.12 B is a DOF for small ranges of motion, but becomes a DOC for larger ranges of motion.

An important question to ask is – what causes the over-constraints that are not recognized by Gruebler's criterion? Any geometric configuration that imposes a certain displacement on a displacement coordinate that corresponds to a DOF is harmless, because the internal forces generated as a result of this geometry are not large enough to affect the compliance of other displacement coordinates. However, if a specific geometric configuration imposes a displacement on a displacement coordinate that corresponds to a DOC, then depending on the magnitude of the imposed displacement, the geometric configuration could

potentially lead to an over-constraint. For example, the imposed displacement in the mechanism of Fig. 3.12B is large enough to generate internal axial forces that affect the transverse stiffness of the two beams. On the other hand, one may consider a geometric arrangement where the platform rotation of the parallelogram flexure in Fig. 13.2A is imposed to be zero. Platform rotation in this case is a direction of DOC, but the actual rotation without the geometric imposition is very small. Despite a large rotational stiffness, the internal forces that are generated in suppressing this rotation are too small to affect the transverse stiffness.

Thus, generally speaking, overconstraint is a consequence of both high stiffness along a DOC, and a relatively large displacement imposed along the DOC, because it is the product of these two factors that results in internal forces which in turn affect compliance and therefore the mobility in the other directions.

The above DOF discussion is based on a choice of finite number of applied forces and a related number of resulting displacements. This discussion is reasonable only in the static case. In the dynamic case, DOF determination becomes even more complicated, because the independent number of displacement variables required to specify the mechanism configuration no longer depends on the number of forces applied. Instead, this number depends on the mode shapes of the structure and the location of the applied forces with respect to these mode shapes. The modes that can be excited by either the actuation forces or disturbance forces determines the DOF in this case. Obviously the number of such modes is infinite, and one needs to select a finite number of these based on the methods of assumed modes, Rayleigh-Ritz or Galerkin. Once again, change in stiffness with applied forces and displacements will affect the mode shapes and therefore can affect the Degrees of Freedom and Constraint in the dynamic case as well.

3.5 Error motions in Flexure Mechanisms

While it is common to treat any undesired displacement of a mechanism as a parasitic motion, a clear generalized definition has not been found in the current literature. We deviate somewhat from this traditional practice and propose a more general description of error motions that has a mathematical basis. Let us assume that the ‘desired’ motion is one that occurs in the direction of the applied force. For any significant displacement to occur, this direction will have to be a DOC. Motions that occurs in any other direction in response to the applied force are deemed as ‘undesirable’. In a purely linear elastic formulation, this has a very simple implication. Keeping in mind that a finite set of forces are allowed, if the compliance matrix that relates these forces to corresponding displacements has any off diagonal terms, then the corresponding forces will lead to undesired motions.

We have already seen that displacements are not necessarily linear elastic in nature. The non-linear formulation presented earlier describes the presence and importance of purely kinematic and elastokinematic displacements. Therefore, from a flexure mechanisms point of view, undesired motion should be determined by first applying a generalized unit loading. This step is important because many effects that result in undesired motions arise in the deformed configuration of a mechanism. From this loaded and displaced configuration, we then vary only that force which is along the direction of primary motion while keeping all others constant, and measure the resulting change in displacements along all the displacement coordinates. All motions other than that in the direction of the applied force are undesired motions.

a) The undesired motions along other Degrees of Freedom are defined here as cross-axis coupling or cross-axes error motions.
b) The undesired motions along the Degrees of Constraint are defined here as parasitic error motions.

Each of these motions can be either purely elastic, or purely kinematic, or elastokinematic, or any combination of these. Let us consider some examples. For a simple beam, if one applies a force along the Y direction, then the displacement δ_x and rotation θ are undesired. Since θ constitutes a DOF direction, the motion is a cross-axis error and is purely elastic in nature. Since δ_x constitutes a DOC direction, it is a parasitic error motion, which has a kinematic as well as an elasto-kinematic component.

In a parallelogram flexure, a pure Y translation is the only desired motion in response to a transverse force; displacement δ_x and rotation θ are undesired. Based on the mobility test presented in the previous section, both δ_x and θ constitute DOC. Therefore the error associated with each of these is a parasitic error. For the case of θ, the parasitic error has a purely elastic component as well as an elastokinematic component. The parasitic error δ_x has a purely kinematic component and also an elastokinematic component.

We next consider a diaphragm flexure presented in Appendix A. It can be shown that this flexure has 3 DOF corresponding to the out of plane motions, and three stiff directions corresponding to the in plane motions. Once again if the center of the flexure is loaded by six generalized forces, and the Z direction force is increased while keeping others constant, there are cross-axis error motions associated with the θ_x and θ_y displacements, which are purely elastic in nature, and parasitic errors in the X, Y and θ_z directions. The former two parasitic errors are elastic and elastokinematic in nature, and the θ_z error is purely kinematic and elastokinematic in nature. The purely kinematic parasitic θ_z is the most prominent of all these.

Similarly, several other examples can be considered. Such a quantification of error terms is important because it reveals what the various components of a given error motion are. Any purely elastic component, whether it appears in a cross-axis error or a parasitic error, may be removed by an appropriate combination of actuation forces. In many cases this simply translates to adjusting the point of force application to provide an additional moment. But kinematic terms that contribute to cross-axes or parasitic errors, are not dependent on forces and therefore may not be eliminated by any combination of forces. The magnitude of these terms may be altered by changing the shape of the constituent flexure building blocks, and a new geometric arrangement involving reversal and symmetry may be necessary to completely eliminate them. Elastokinematic terms are influenced by both of these two schemes – by adding actuation forces and by making geometric changes. This provides the designer important information regarding the kind of optimization and topological redesign that might be needed to improve the motion accuracy in a flexure mechanism.

3.6 Energy Methods

Instead of solving the equations of force equilibrium, geometric equilibrium and constitutive relationships explicitly, as done in this chapter, one may instead make use of energy methods. There are two theorems that form the basis for all energy methods, the Principle of Virtual Work and the Principle of Complimentary Virtual Work [78-79].

The Principle of Virtual Work (PVW) is fundamentally a necessary and sufficient statement for the conditions of force equilibrium, without any restrictions on its applicability. In statics, the Principle of Minimum Potential Energy and Castigliano's Second Theorem may be derived from the PVW for the specific case of conservative systems. Furthermore, in conjunction with d'Alembert's Principle, the PVW becomes the basis for Hamilton's formulations in dynamics.

Similarly, the Principle of Complimentary Virtual Work is a necessary and sufficient statement for the conditions of geometric equilibrium, with some restrictions. The Principle of Minimum Complimentary Potential Energy and Castigliano's First Theorem are a direct consequence of the PCVW. Although not as commonly used, complimentary formulations in dynamics originating from the PCVW have also been developed [80] .

Although it is generally considered that the these two theorems offer a perfect symmetry and duality in formulation, the latter is actually a much weaker statement as compared to the first. There are two reasons that make the PVW more robust than the PCVW, and these are explained in the following paragraphs.

While solving a problem in mechanics, one is often interested in determining only the external force-displacement characteristics, and not the internal forces and displacements. Vector methods based on Newton's Laws involve all internal forces and displacements, thus making the process computationally tedious. Energy methods offer an alternate to the vector methods, by excluding the internal forces from the formulation.

Let us briefly look at the duality that exists between force equilibrium (or compatibility) and geometric constraints (or compatibility). For the sake of illustration, we consider a system with rigid geometric constraints. In such a system, it is the internal forces that enforce geometric compatibility, and it is because of geometric constraints that internal forces arise. In fact, internal forces are aligned along the direction of the corresponding geometric constraints. Given a system in a state of deformation under a set of external loads, this relationship between internal forces in equilibrium and geometric compatibility is well evident.

The principles of energy build upon virtual variations from this loaded and deformed configuration. In the presence of virtual displacements, which are defined as small variations in the real displacements that do not violate the conditions of geometric compatibility, the work done by the internal forces associated with the rigid constraints is zero. During these displacement variations, time is assumed frozen and forces remain unchanged – hence the name 'virtual'. Since the virtual displacements cannot violate the geometric constraints, and since internal forces are aligned along the geometric constraints, the virtual displacements are orthogonal to the geometric constraints as well as the corresponding internal forces. It is because of this orthogonality between virtual displacements and internal forces, the internal forces do no virtual work, and therefore are eliminated from the principle of virtual work formulation.

The other possible variation is one that can be made to the applied forces such that these variations obey force equilibrium and do not affect the real displacements. The Principle of Complimentary Virtual Work also attempts to exclude the internal forces by considering real displacements and virtual forces, but a problem arises in making a generalization. This is due to the fact that conditions of geometric constraints can be non-linear in the displacement variables. This implies that, while differential displacements are orthogonal to internal forces, real displacements need not be so. Thus, the computation of complimentary virtual work by taking a scalar product of real displacements and virtual forces does not always result in an elimination of internal force dependent terms. Since force equilibrium conditions are necessarily linear in the force terms, the true internal forces and the differential virtual internal forces are always are in the same direction. On the other hand, displacements and differential virtual displacements are proportional, or collinear, only when the conditions of geometric compatibility are linear in displacement terms. In many large displacement problems, this is not the case. The resulting loss of orthogonality between real

displacements and virtual forces restricts the applicability of PCVW to problems that are geometrically linear, or ones where the true displacements are small enough to justify a linear approximation of the geometric constraints. For the reasons explained above, no such issue arises in the case of the Principle of Virtual Work, thus making it far more robust and versatile as compared to its sibling.

The second problem associated with the PCVW is the lack of an absolute reference for displacements, which leads to ambiguity in the definition for Complementary Virtual Work. On the other hand, PVW is immune to this because neither forces nor differential virtual differential displacements require a reference frame.

For these reasons, one has to exercise caution in the use of PCVW. In fact all the successful applications of complementary principles are not really based on the PCVW but instead are indirectly derived from the PVW [80-81]. For the purpose of this research, PVW work was applied for the uniform beam discussed in Section 3.1, and results identical to expressions 3.9 and 3.10 were obtained. Clearly this is a situation where the conditions for geometric compatibility are non-linear, and therefore a direct application of PCVW resulted in incorrect expressions, as expected. A complementary formulation similar to [81], based on PVW, was not but can be attempted.

The preceding sections have highlighted the importance of overconstraint and error motions in flexure mechanisms. Overconstraint is a direct consequence of internal forces, whereas some components of error motions are a consequence of geometric constraints. While energy methods capture both these effects very well, and although the PVW is applicable in this case, there are two reasons why we decide to not utilize it for the subsequent analyses.

1. PVW yields the final results in the form of forces expressed in terms of displacements. Because of non-linearities involved, it is extremely tedious to invert these relations to obtain displacements in terms of forces which is what is ultimately desired in this analysis.
2. Contrary to what is commonly understood, an unusual geometric compatibility condition is encountered in the non-linear beam bending analysis. Normally, geometric compatibility is purely a relationship between the various displacement variables in the system. In this case, the condition of geometric constraint (3.13) actually has a force term explicitly embedded in it. While the PVW is still applicable but its usefulness in terms of eliminating the internal forces is somewhat diminished because one still needs to include the internal axial force p in the formulation of the beam to obtain virtual displacements.